ESR and ENDOR Studies of the π Cation Radical of Bacteriochlorophyll[1]

D. C. Borg,* A. Forman,* and J. Fajer*

Contribution from The Medical Research Center and Department of Applied Science, Brookhaven National Laboratory, Upton, New York 11973. *Received April 5, 1976*

Abstract: Chemical oxidation of bacteriochlorophyll (BChl) in nonaqueous solvents, under rigorously anaerobic and anhydrous conditions, yields a stable cation radical ($BChl^{\cdot+}$). This species, investigated by computer-assisted magnetic resonance techniques, displays, at 0 °C, partially resolved ESR spectra and reveals, through high power ENDOR, at least seven proton hyperfine splittings. The latter are assigned on the basis of reported molecular orbital calculations, selective deuterations, and model compound studies, and the assignments are supported by reconstruction of the experimental ESR spectra of both protonated and deuterated $BChl^{\cdot+}$. Predictions based on these same assignments for the overall line widths of the Gaussian singlet ESR spectra to be expected for both protonated and deuterated $P870^{\cdot+}$ (the oxidized form of BChl in vivo) are also in good agreement with reported experimental values. Hence the new data provide further support for the dimer model of BChl as the primary electron donor in bacterial photosynthesis and, in addition, help define the electronic configuration of the P870 radical.

Although the primary electron donor species of green plant and bacterial photosynthesis have long been detected by ESR,[2] much remains to be done in characterizing these components in order to understand better their interactions and to elucidate more fully the mechanisms underlying the photochemical and physical steps of photosynthesis. It is generally accepted that the main ESR signal observed originates from light-induced one-electron oxidation of chlorophyll in a special environment, the photoreaction center, giving rise to a free radical from bacteriochlorophyll (BChl) in photosynthetic bacteria or from chlorophyll a (Chl) in chloroplasts of green plants and algae.[3-8] Because the ESR signals observed in vivo are narrower by the square root of two (as predicted for a dimer) than those obtained from the respective free radicals in vitro,[8,9] it has been concluded that within the reaction centers of purple bacteria (P870) and plants (P700) the unpaired electrons of the free radicals delocalize over "special pairs" of chlorophyll molecules, each pair bridged by a water molecule or other bifunctional ligand. Spin delocalization over such a pair of BChl or Chl is also consistent with the effect of ^{13}C substitution on the ESR line,[10] the small zero-field parameters from triplet states of BChl,[11] and the halving of several hyperfine constants obtained by ENDOR from chlorophyll radicals in vivo compared with $BChl^{\cdot+}$ or $Chl^{\cdot+}$ in vitro.[12-14]

Despite the determination of a few hyperfine couplings from ENDOR of frozen and selectively deuterated samples,[12-14] the inability, heretofore, to resolve spectral structure from the Gaussian singlet ESR signals of $BChl^{\cdot+}$ or $Chl^{\cdot+}$ has precluded identification of the paramagnetic centers by the usual method of analyzing the number, amplitude, and splitting of ESR hyperfine lines,[4-6,8,15] thus leaving the electronic structures of these important radicals obscure. Nevertheless, the π cation nature of light-induced or chemically oxidized reaction centers has been established by strong similarities in their ESR and optical properties to those of π cation radicals formed chemically,[16] a conclusion previously inferred from the effects of various isotopic substitutions upon ESR signal widths in vitro and in vivo.[3-6,8,10,17,18]

We now report resolved structural detail from the ESR spectra of $BChl^{\cdot+}$ and $BPh^{\cdot+}$ (the cation radical of bacteriopheophytin) and the measurement of seven protonic splitting constants from the ENDOR data. Guided by our previous studies of π cation radicals of selectively deuterated bacteriochlorin model compounds,[19] we assign hyperfine coupling constants and construct computer simulations that match satisfactorily the observed ESR spectra. The results are in accord with molecular orbital calculations and the model work in attributing small splittings (~1 G) to the four nitrogen atoms and in revealing large proton splittings on the saturated rings (3.7-5.8 G). In addition, the methyl proton splittings from $BChl^{\cdot+}$ in solution (1.7-3.4 G) differ little from those of frozen samples[12-14] as expected if the methyl groups are free to rotate. The experimental in vitro data extrapolated to predict in vivo results yield good agreement with the dimer model of $P870^{\cdot+}$ for both protonated and deuterated bacteria.

Experimental Section

ESR spectra were obtained on a Varian E-12 X-band spectrometer using low microwave powers (1 mW) and low modulation amplitudes (0.5 G). Temperature was controlled with a Varian E-257 accessory. Spectra were swept in 30 s, and the data from multiple scans (typically a few hundred to 2000) were collected and averaged on an SDS Sigma 2 computer. The field sweeps were ramped by the computer, while drifts in field or klystron frequency were compensated for by using the Varian E-272 field-frequency accessory in the marker mode. The marker signal from a reference free radical was located in the first scan, and subsequent data were automatically shifted into the data-summing memory buffer so as to keep the field-frequency marker in the same channel.

ENDOR spectra were taken with the Varian E-700 high power ENDOR accessory, using a cylindrical TE_{011} mode, wide-stack ENDOR cavity for frozen samples and an E-1737 cavity which provides large rf fields (~40 G in the rotating frame) for samples in liquid solution. The low-field side of the power-saturated ESR spectrum was monitored, and spectra were collected on a Northern Scientific NS 575 signal averager before transfer to the Sigma 2 computer. The rf frequency counter of the E-700 ENDOR accessory was used to drive the stepping motor of the E-12 spectrometer's recorder so that ENDOR spectra linear in frequency were obtained. The NS 575 was modified so that its channel advance could also be driven by the pulses of the same stepping motor, thus providing linear digitized ENDOR scans as well. Multiple scans were synchronized by triggering the NS 575 from the frequency counter.

The preparation of BChl, $ZnTPP^{\cdot+}ClO_4^-$ (zinc tetraphenylporphyrin perchlorate, a free radical), and $(FeTPP)_2O^+ClO_4^-$ (μ-oxo dimer of iron tetraphenylporphyrin perchlorate, an oxidized salt) as well as the purification of solvents have been described.[19,21] ESR samples were prepared on a greaseless vacuum line with previously dried and out-gassed solvents. An oxidizing agent, $ZnTPP^{\cdot+}ClO_4^-$, $(FeTPP)_2O^+ClO_4^-$, or I_2, was introduced into compartment A of the ESR ampule (Figure 1), which was then pumped out and sealed. BChl was introduced into compartment C and the tube pumped out. CH_2Cl_2 was condensed into C to dissolve the BChl, the solvent was distilled out, and the BChl was dried in vacuum. Fresh solvent was condensed into C, the system was pumped out, and the sample was sealed at B. The BChl could be oxidized, on demand, by breaking the glass seal which delineates compartment A and dissolving the oxidizing agent.

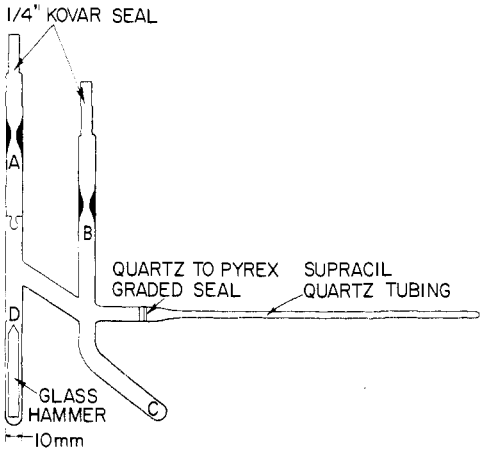

Figure 1. Sample ESR and ENDOR tube.

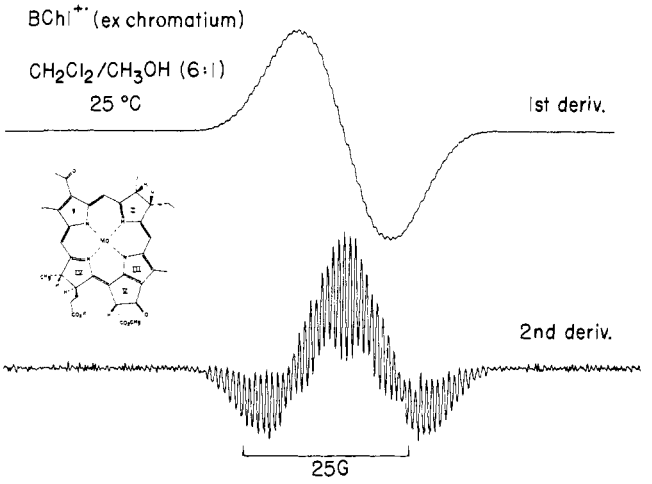

Figure 2. First and second derivative ESR spectra of $BChl^{\cdot+}$ extracted from *C. vinosum* at 25 °C.

The concentration of resultant radical could be varied infinitely: the solution was divided between compartments D and C and all the solvent condensed from D into C by cooling C.

If the preparation was reversed and $ZnTPP^{\cdot+}ClO_4^-$ was introduced in C and an excess of BChl in A, comparison of radical concentrations before and after the oxidation of BChl could be made on the same sample. Radical concentrations were found to agree within 10%. The identity of the $BChl^{\cdot+}$ radical was also verified spectorphotometrically on the same sample by the addition of an optical absorption cell to the ESR apparatus.

Results

Oxidation of BChl in chloroform, dichloromethane, and mixtures of dichloromethane:methanol (6:1) yielded free radicals that remained stable for many days. Under more "usual" ESR operating conditions (microwave power > 1 mW, modulation amplitude ≥ 1 G, or failure to rigorously exclude oxygen) only Gaussian singlet ESR spectra were recorded. However, under the restrictions defined in the Experimental Section, and after signal averaging, partially resolved spectra with 50 or more lines were obtained. The resolution was further enhanced by the computer-derived second derivative presentation. Figure 2 displays results of this kind obtained with BChl extracted from *Chromatium vinosum* in dichloromethane:methanol. Sufficient spectral detail was resolved from *C. vinosum* BChl oxidized in other solvents to demonstrate that the hyperfine splitting (hfs) pattern, although similar, was not identical and thus was solvent dependent (Figure 3), as we observed previously for cation radicals of bacteriochlorins.[19]

Chromatium vinosum contains the fatty alcohol, phytol, as

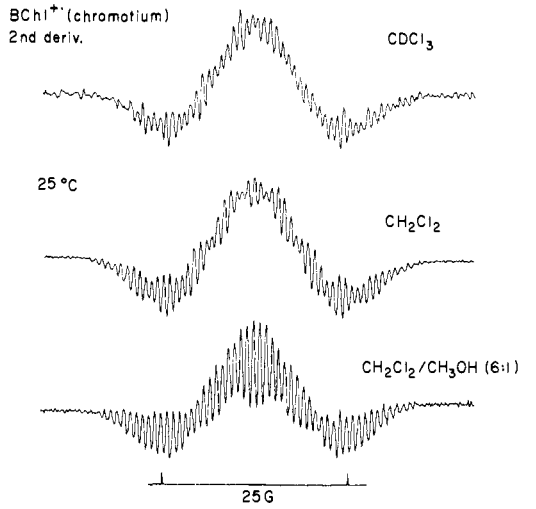

Figure 3. Comparison of second derivative ESR spectra of $BChl^{\cdot+}$ (*C. vinosum*) in different solvents at 25 °C.

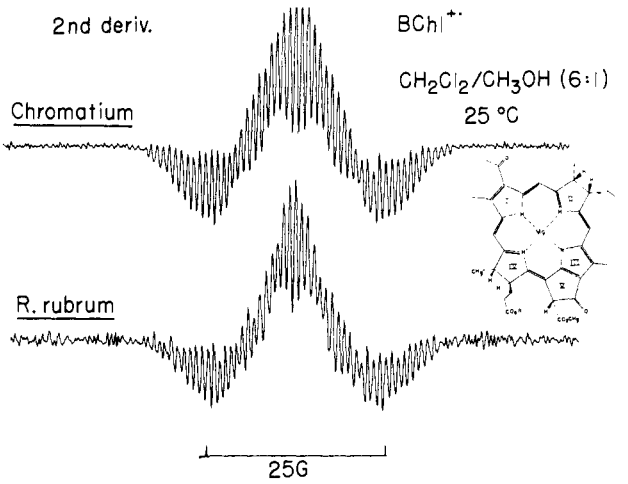

Figure 4. Second derivative ESR spectra of $BChl^{\cdot+}$ extracted from *C. vinosum* (top) and *R. rubrum* (bottom) at 25 °C.

the long hydrophobic side chain (R in Figure 4). In BChl extracted from *Rhodospirillum rubrum*, R = geranylgeranyl, yet the ESR spectra from the respective $BChl^{\cdot+}$ radicals are essentially the same (Figure 4). Despite some differences in the second derivative spectral envelopes, the line positions and widths correspond well (Figure 4), and we conclude that the side chain R has no significant effect on the distribution of the unpaired electron density. (Replacement of the phytyl by an ethyl group in Chl similarly yields no distinguishable change in the first derivative singlet ESR spectra of $Chl^{\cdot+}$.[16])

To assure that the hfs observed did not arise from impurities or decomposition products, BChl samples were chromatographed just before use, BChl preparations from three other laboratories were tried, and three different oxidizing agents were employed. None of these precedures altered the hfs. Furthermore, since the oxidation potential of BPh exceeds that of BChl[19] and is beyond the reach of iodine oxidation, the results with iodine minimize the possibility that the hfs attributed to $BChl^{\cdot+}$ (Figures 2-4) derive from contaminating $BPh^{+\cdot}$ (Figure 7).

ENDOR spectra of *C. vinosum* $BChl^{\cdot+}$ frozen in dichloromethane:methanol at −170 °C display two major peaks, a higher-frequency unresolved spectral "wing", and a small splitting surrounding the matrix signal at the free proton resonance frequency, ν_H (Figure 5).

In contrast to the results from frozen samples, data taken

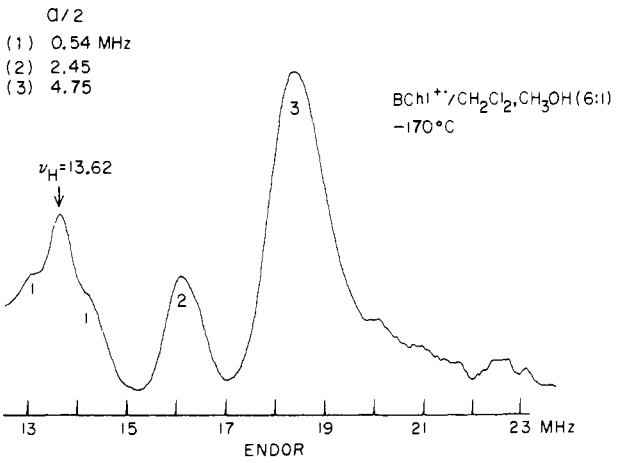

Figure 5. ENDOR spectrum of $BChl^{\cdot+}$ (*C. vinosum*) at −170 °C.

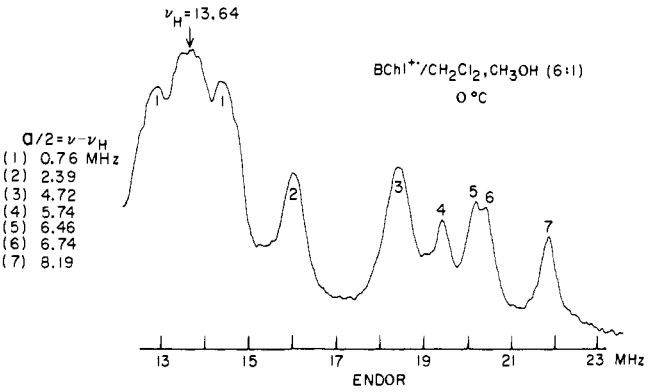

Figure 6. ENDOR spectrum of $BChl^{\cdot+}$ (*C. vinosum*) at 0 °C.

from $BChl^{\cdot+}$ in fluid solution at 0 °C in the high-rf power ENDOR cavity reveal seven clearly resolved lines (Figure 6).

A fully deuterated (~99%) sample of BChl extracted from *R. rubrum* was received from J. J. Katz. We noted with reference to Figure 4 that the line width and resolved hfs of $BChl^{\cdot+}$ form *R. rubrum* and *C. vinosum* are essentially the same. Hence the ESR spectra of deuterated $BChl^{\cdot+}$ from either species should be comparable, and we found for the deuterated $BChl^{\cdot+}$ from *R. rubrum* ΔH = 5.0 G, where ΔH is the peak-to-peak line width of the first derivative singlet.

Oxidation of bacteriopheophytin, BPh, the free base of BChl, yields the ESR and ENDOR spectra shown in Figure 7. The first derivative singlet[19] is 14.4 G wide in CH_2Cl_2 and 14.0 G in $CHCl_3$ vs. values of 13.2 and 12.8 for $BChl^{\cdot+}$ in the same solvents. Feher et al. prepared $BPh^{\cdot+}$ by oxidation with $SnCl_4$ in CH_2Cl_2 and found ΔH = 13 G at 80 K with an ENDOR transition equivalent to a_H = 2.1 G.[13] As shown in Figure 7, at least two transitions are observed at 100 K in frozen methanol with a_H = 1.9 and 3.4 G (with a possible third splitting, $a_H \sim 0.3$ G).

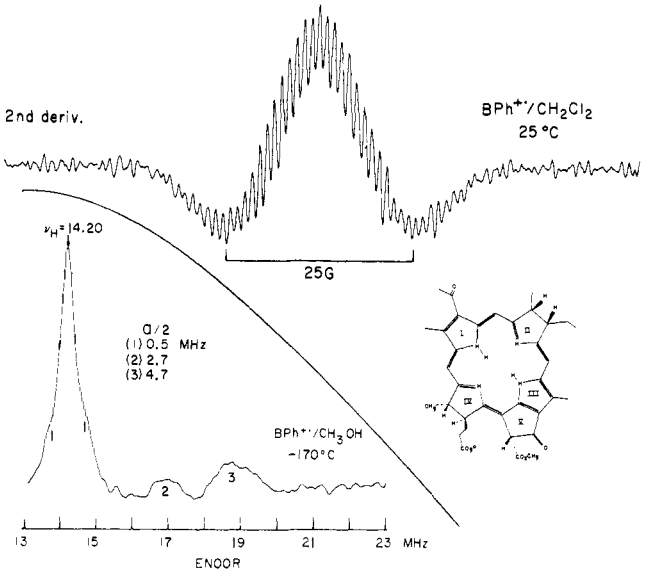

Figure 7. Second derivative ESR spectrum at 25 °C and ENDOR spectrum at −170 °C of $BPh^{\cdot+}$ (*C. vinosum*).

Discussion

The ENDOR spectra of frozen $BChl^{\cdot+}$ from *C. vinosum* (Figure 5) resemble closely those found previously from *R. rubrum* by Norris et al.[12,14] They measured splittings of 1.4, 5.2, and 9.8 MHz plus unresolved resonances corresponding to splittings of ~14 MHz (2.8 MHz = 1 G), which compare favorably with our values of 1.1, 4.9, and 9.5 MHz with a spectral wing from splittings of >14 MHz. Subsequently Feher and colleagues[13] reported for $BChl^{\cdot+}$ (*R. spheroides*) two splittings at 5.0 and 9.2 MHz with unresolved ENDOR structure from splittings of ~16 MHz. ENDOR peaks (1), (2), and (3) of $BChl^{\cdot+}$ in solution (Figure 6) with a = 1.5, 4.8, and 9.5 MHz, respectively, can therefore be identified with the ENDOR lines resolved from frozen $BChl^{\cdot+}$ (Figure 5). The two largest of these were assigned to the protons of methyl groups at C-1 (on ring I) and C-5 (on ring III) on the basis of selective deuteration.[12,13] Other deuterations led Norris et al.[14] to attribute the small ENDOR splitting [peak (1)] to the α, β, δ methine protons and/or to the proton on C-10 in ring V.

We assign the four additional lines resolved from solution ENDOR of $BChl^{\cdot+}$ [peaks (4), (5), (6), and (7) of Figure 6] to the four protons 3, 4, 7, and 8 on rings II and IV on the basis of the molecular orbital calculations of Otten[20] and Felton,[19] which predict large spin densities at the α carbons of these saturated rings. The predictions are supported by our studies of radicals of zinc tetraphenylbacteriochlorin (a model for bacteriochlorophyll) which show well resolved hfs that can be unambiguously assigned by selective deuteration to the β protons of the saturated rings with a_H = 7.5 G in CH_2Cl_2.[19] Identification of the four large splittings with the β protons of rings II and IV is further verified by the findings of Feher et al.[13] that oxidized chromatophores from bacteria grown in D_2O and succinic acid, which results in deuterium replacement of these protons, causes the unresolved large ENDOR splitting(s) from frozen $BChl^{\cdot+}$ to disappear. These poorly resolved ENDOR features are the counterpart of the four peaks resolved at 0 °C reported here (Figure 6), where the tumbling of molecules in solution averages out the anisotropies that broaden lines in the immobilized samples.

In the model bacteriochlorin compounds with their twofold axes of symmetry, all β-proton splittings from the saturated pyrrole rings are equal,[19] whereas four different β proton coupling constants are found, not surprisingly, in $BChl^{\cdot+}$, since rings II and IV are different, chlorophylls are not entirely planar,[22,23] and the molecule is significantly asymmetrical. These factors, presumably also the source of the unequal methyl group splittings (which become essentially equal upon rupture of the exocyclic ring V[14]), could cause unequal delocalization of the unpaired electron at the carbons in the π systems and different dihedral angles, θ, for the different β protons, where θ is the angle between the $2p_z$ orbital of the α carbon atom, C_α, and the C_α, C_β, H_β plane.

The splitting constant of the β protons is given by $a_H \simeq \text{const}(\rho_C \cos^2 \theta)$, where ρ_C is the spin density on the α carbon

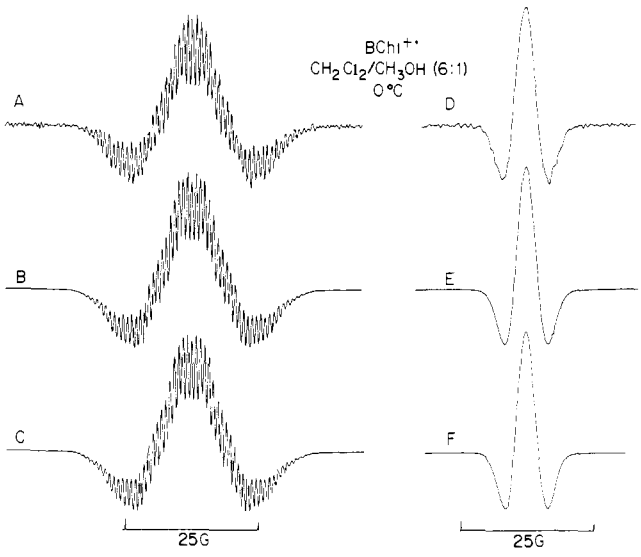

Figure 8. (A) Second derivative ESR spectrum of $BChl^{\cdot+}$ (*C. vinosum*) at 0 °C. (B) Computer simulation of A, Lorentzian line shape, 0.8 G line width, 1 proton 4.10 G, 1 proton 4.62, 1 proton 4.82, 1 proton 5.84, 3 protons 1.71, 3 protons 3.37, one nitrogen 1.12, 3 nitrogens 0.78, 1 proton 0.54 G. (C) Simulation of A, 0.6 G line width, with three, instead of one, protons 0.54 G. (D) Second derivative ESR spectrum of perdeuterio $BChl^{\cdot+}$ (*R. rubrum*). (E) Simulation of D; all proton splittings in simulation B have been converted to deuteron splittings ($a_D/a_H = 0.1535$). (F) Deuterated equivalent of simulation C.

of the π system. For a freely rotating methyl group $\cos^2\theta$ averages to 0.5 and $a_H = 39\rho_C$.[24,25] Assuming an average dihedral angle of ~45° (from the x-ray data on ethyl chlorophyllides a and b[22,23]) the spin densities at the saturated carbons of rings II and IV range between 0.1 and 0.15. The spin densities on the carbons carrying the methyl groups in rings I and III are 0.044 and 0.086, respectively, while the methine carbons (α, β, δ) carry ~0.002 density units (from the McConnell equation for α protons: $a_H = 27\rho_{C_\alpha}$[26]). Using the least sophisticated equation for nitrogen couplings,[27] $a_N = 32\rho_N$, the nitrogen atoms carry ~0.03–0.04 units. Approximately 50% of the unpaired spin density is thus localized at the α carbons of rings II and IV. Since neither the nitrogens nor the methine positions carry large densities, the remainder of the unpaired electron distribution must be in rings I and III.

The resolved ESR spectra from $BChl^{\cdot+}$ (Figures 2–4) provide a test for the assignments made from the ENDOR analysis. Simulated second derivative spectra respond sensitively to small variations in assumed line shapes or widths, as well as to the number and values of hyperfine splittings assumed, so that accurate matching of the hfs features provides demanding criteria by which to judge goodness of fit.

Figure 8A shows the second derivative ESR spectrum of $BChl^{\cdot+}$ from *C. vinosum* at 0 °C, the temperature at which the solution ENDOR was carried out. The following hyperfine splitting constants were taken from the ENDOR: four β protons with $a_H = 4.10$, 4.62, 4.82, and 5.84 G, and two sets of three methyl-group protons, with $a_{CH_3} = 1.71$ and 3.37 G. ENDOR transition (1) may represent as many as four protons, three methine and C-10. Accordingly, trial simulations utilizing one, two, three, or four protons of $a_H = 0.54$ G were attempted, but for all reasonable nitrogen splitting constants (*vide infra*), only assumptions of one or three protonic splittings of 0.54 G resembled the experimental spectra.

Trial values of nitrogen splitting constants were set by the inferential evidence of McElroy et al.,[5] who deduced $a_N \sim 1.2$ G for $BChl^{\cdot+}$ based on the narrowing of its ESR envelope upon deuteration, and by the nitrogen splittings, $a_N \sim 1.1$ G, we found for cation radicals of zinc and free base tetraphenylbacteriochlorin (H_2TPBC).[19] Making the nitrogens inequivalent improved the fit regardless of whether one or three protons with $a_H = 0.54$ G were assumed. Simulations based on four different β proton splittings and two methyl groups, plus four nitrogens (one inequivalent), are compared with the actual ESR in Figure 8, assuming either one (Figure 8B) or three (Figure 8C) protons with $a_H = 0.54$ G. The above trial functions also fit accurately the first derivative spectra of both protonated species, even out to where the spectral wings are <1% of peak height. Reasonable simulations can thus be achieved with a minimum of guesswork with most of the inputs set directly by experimental data or estimated from model compounds. Not all possible sites of interaction with the unpaired electron have been detected by ENDOR or entered into the simulations, however. For example, the methyl and methylene protons of rings II and IV should contribute to the ESR spectrum. Because these are γ protons, twice removed from carbon centers with π spin density, their contributions are expected to be small. (The γ proton splittings obtained from the resolved ESR spectrum of the cation radical of zinc *meso*-tetraethylporphyrin[24] are an order of magnitude less than the adjacent β splittings.) Presumably these and other small splittings are subsumed in the Lorentzian line widths of 0.6–0.8 G used in the simulations.

A further check on the validity of the values of a_N and a_H used in the simulations is given by comparing the predicted and experimental spectra for perdeuterio BChl (Figure 8D). The simulations of Figures 8E and 8F replace doublet proton splitting centers with triplet deuteron centers where $a_D/a_H = 0.1535$, with all other inputs held constant. The results confirm that the assignments based on ESR and ENDOR results are eminently reasonable.

Simulations of ESR spectra for $BPh^{\cdot+}$ required more guesswork than was the case for $BChl^{\cdot+}$. The similarities between the detected ENDOR transitions (presumably from rotating methyl groups) in frozen $BChl^{\cdot+}$ (Figure 5) and $BPh^{\cdot+}$ (Figure 7) are consistent with the small differences in ESR splittings between metallated and free base bacteriochlorin cation radicals.[19] A number of trial simulations, which include methyl splittings ($a_{CH_3} = 1.9$ and 3.4 G), four large β protons ($a_H \sim 4$–6 G, one inequivalent), four nitrogens ($a_N \sim 1$ G), and meso protons ($a_{H_{meso}} \sim 0.3$ G) all yield verisimilar versions of the experimental $BPh^{\cdot+}$ spectrum. These agree with both the $H_2TPBC^{\cdot+}$ data and the MO calculations but are only tentative since the β protons have not been observed by ENDOR. Large β protons are clearly required to account for the overall line width of the spectrum of $BPh^{\cdot+}$. Moreover, the trend shown in the model bacteriochlorin compounds, i.e., that the β proton splittings are larger and solvent dependent in the free base, is supported by the experimental ΔH for $BPh^{\cdot+}$ vs. those for $BChl^{\cdot+}$, if the change in ΔH is attributed to the β protons.[19] Additional support for these assumptions was found in the spectrum of $BPh^{\cdot+}$, ~90% deuterated, which displays ΔH of 5.8 G vs. a line width of ~5.2 G computed for 100% deuteration.

Hyperfine splitting constants reflect the electron densities at various nuclei, and our determination of these values thus allows a mapping of the electronic structures of $BChl^{\cdot+}$ and related compounds. If the dimeric model of BChl in the photoreaction center is correct, our assignments should also predict splittings and overall line widths of spectral envelopes in vivo, based upon halving the hfs parameters for the monomer and doubling the number of splitting centers. The calculated ΔH values (obtained by filtering the simulated spectra on the computer until resolution just disappears) for the $P870^{\cdot+}$ dimer in vivo are 9.3 and 3.4 G for protons and deuterons, respectively. Actually found were 9.4 ± 0.2 and 3.9 ± 0.2 G for *R. rubrum*.[5] A range of values reported for ΔH of $P870^{\cdot+}$ (9.4–9.7 G) from various microorganisms[3-5,8,13,15,17] could

be explained by altered local environments in the different reaction centers, because we have shown that solvent changes can modify the hyperfine splittings of bacteriochlorophyll and bacteriochlorins.[19] The agreement between calculated and observed values of ΔH for $P870^{\cdot+}$ alone does not distinguish between the slightly different dimeric models proposed by Norris et al.,[14,31] Boxer and Closs,[32] and Fong[28] for P870.

In the initial photoact of bacterial photosynthesis it is postulated that P870, donates, in less than 10 ps,[29] an electron to a nearby BPh to yield its anion radical[30] and $P870^{\cdot+}$. The latter is eventually reduced (in microseconds) by electron transfer from cytochrome c_2 which, in turn, may also function via a porphyrin radical.[21,33] The spin density profiles provided by ESR and ENDOR have, therefore, now allowed the electron distribution of the free radical species involved in the very first and last stages of cyclic electron transport in bacterial photosynthesis to be described in some detail. Because these radicals must be fixed in close proximity, the extent of overlap (or lack of it) between their electronic configurations must influence the rates of electron transfer between them.

References and Notes

(1) This work was performed under the auspices of the U.S. Energy Research and Development Administration
(2) P. A. Loach and B. J. Hales. "Free Radicals in Biology", W. A. Pryor, Ed., Academic Press, New York, N.Y., 1976, p 199.
(3) J. D. McElroy, G. Feher, and D. C. Mauzerall, *Biochim. Biophys. Acta*, **172**, 180 (1969).
(4) D. H. Kohl, "Biological Applications of Electron Spin Resonance", H. M. Swartz, J. R. Bolton, and D. C. Borg, Ed., Wiley-Interscience, New York, N.Y., 1972, p 213.
(5) J. D. McElroy, G. Feher, and D. C. Mauzerall, *Biochim. Biophys. Acta*, **267**, 363 (1972).
(6) M. E. Druyan, J. R. Norris, and J. J. Katz, *J. Am. Chem. Soc.*, **95**, 1682 (1973).
(7) J. D. McElroy, D. C. Mauzerall, and G. Feher, *Biochim. Biophys. Acta*, **333**, 261 (1974).
(8) J. T. Warden and J. R. Bolton, *Acc. Chem. Res.*, 7, 189 (1974).
(9) J. R. Norris, R. A. Uphaus, H. L. Crespi, and J. J. Katz, *Proc. Natl. Acad. Sci. U.S.A.*, **68** 625 (1971).
(10) J. R. Norris, R. A. Uphaus, and J. J. Katz, *Biochim. Biophys. Acta*, **275**, 161 (1972).
(11) R. A. Uphaus, J. R. Norris, and J. J. Katz, *Biochem. Biophys. Res. Commun.*, **61**, 1057 (1974).
(12) J. R. Norris, M. E. Druyan, and J. J. Katz, *J. Am. Chem. Soc.*, **95**, 1680 (1973).
(13) G. Feher, A. J. Hoff, R. A. Isaacson, and L. C. Ackerson, *Ann. N.Y. Acad. Sci.*, **244**, 239 (1975).
(14) J. R. Norris, H. Scheer, M. E. Druyan, and J. J. Katz, *Proc. Natl. Acad. Sci. U.S.A.*, **71**, 4897 (1974).
(15) J. R. Harbour and G. Tollin, *Photochem. Photobiol.*, **19**, 69 (1974).
(16) D. C. Borg, J. Fajer, R. H. Felton, and D. Dolphin, *Proc. Natl. Acad. Sci. U.S.A.*, **67**, 813 (1970).
(17) D. H. Kohl, J. Townsend, B. Commoner, H. L. Crespi, R. C. Dougherty, and J. J. Katz, *Nature (London)*, **206**, 1105 (965).
(18) J. J. Katz, K. Ballschmiter, M. Garcia-Morin, H. H. Strain, and R. A. Uphaus, *Proc. Natl. Acad. Sci. U.S.A.*, **60**, 100 (1968).
(19) J. Fajer, D. C. Borg, A. Forman, R. H. Felton, D. Dolphin, and L. Vegh, *Proc. Natl. Acad. Sci. U.S.A.*, **71**, 994 (1974).
(20) H. A. Otten, *Photochem. Photobiol.*, **14**, 589 (1971).
(21) J. Fajer, D. C. Borg, A. Forman, R. H. Felton, L. Vegh, and D. Dolphin, *Ann. N.Y. Acad. Sci.*, **206**, 349 (1973).
(22) C. E. Strouse, *Proc. Natl. Acad. Sci. U.S.A.*, 71, 325 (1973).
(23) (a) H.-C. Chow, R. Serlin, and C. E. Strouse, *J. Am. Chem. Soc.*, **97**, 7230 (1975); (b) R. Serlin, H.-C. Chow, and C. E. Strouse, *ibid.*, **97**, 7237 (1975).
(24) J. Fajer, D. C. Borg, A. Forman, A. D. Adler, and V. Varadi, *J. Am. Chem. Soc.*, **96**, 1238 (1974).
(25) G. Vincow, "Radical Ions", E. T. Kaiser and L. Kevan, Ed., Interscience, New York, N.Y., 1968, p 151.
(26) H. M. McConnell, *J. Chem. Phys.*, **24**, 764 (1956).
(27) J. R. Bolton, A. Carrington, and J. dos Santos-Veiga, *Mol. Phys.*, **5**, 465 (1962).
(28) F. K. Fong, "Theory of Molecular Relaxation", Wiley-Interscience, New York, N.Y., 1975, p 241.
(29) P. L. Dutton, K. J. Kaufmann, B. Chance, and P. M. Rentzepis, *FEBS Lett.*, **60**, 275 (1975).
(30) J. Fajer, D. C. Brune, M. S. Davis, A. Forman, and L. D. Spaulding. *Proc. Natl. Acad. Sci. U.S.A.*, **72**, 4956 (1975).
(31) L. Shipman, T. M. Cotton, J. R. Norris, and J. J. Katz, *Proc. Natl. Acad. Sci. U.S.A.*, **73**, 1791 (1976).
(32) S. G. Boxer and G. L. Closs, *J. Am. Chem. Soc.*, **98**, 5406 (1976).
(33) J. Fajer and M. S. Davis, "The Porphyrins", D. Dolphin, Ed., Academic Press, New York, N.Y., in press.

^{13}C NMR Studies of 9-Methyl-9-azabicyclo[3.3.1]nonane and Related Compounds

S. F. Nelsen,* G. R. Weisman, E. L. Clennan, and V. E. Peacock

Contribution from the Department of Chemistry, University of Wisconsin, Madison, Wisconsin 53706.

Received March 19, 1976

Abstract: The ^{13}C NMR spectra for 9-methyl-9-azabicyclo[3.3.1]nonane (**1**) and 2-methyl-2-azaadamantane (**2**) were studied at low temperature. Comparison with the related hydrocarbons (N replaced by CH) reveals that the β carbons anti to the nitrogen lone pair are shifted upfield 1–2 ppm more than the syn carbons. Inversion barriers for **1** and **2** were determined by line shape analysis to be about 8.1 kcal/mol at −90 °C. 9-Dimethylamino-9-azabicyclo[3.3.1]nonane (**3**) showed no evidence for preferential line broadening to −132 °C, and must have a considerably lower barrier for nitrogen inversion.

Although considerable progress is being made in the interpretation of ^{13}C NMR chemical shifts, the sorting out of the various effects involved in molecules containing heteroatoms is a complex problem.[1] Reasonably consistent correlations were observed by Eggert and Djerassi[2] for a series of aliphatic amines when the observed chemical shifts were compared to those of the related hydrocarbons (N replaced by CH), and shift parameters were devised. Shift parameters which work for acyclic systems are known not to transfer successfully to cyclic ones, because of important conformational effects upon ^{13}C shifts. Several studies of carbon shifts of the most widespread class of cyclic amines, the piperidines, have appeared,[3-7] but these studies have not allowed answering a key question in the whole area of ^{13}C NMR of heteroatomic molecules, the size of the effect of lone pair configuration upon ^{13}C chemical shifts. We report here variable temperature studies on bi- and tricyclic piperidines in which nitrogen inversion is slow at low temperature, and in which both axial and equatorial lone pairs are present, allowing measurement of both the chemical shift changes with lone pair configuration and the activation parameters for nitrogen inversion in these systems.

Results

The NMR spectra for 9-azabicyclo[3.3.1]nonane derivatives